Carbohydrate Polymers 96 (2013) 522–527

Contents lists available at SciVerse ScienceDirect

Carbohydrate Polymers

journal homepage: www.elsevier.com/locate/carbpol

A novel high mechanical strength shape memory polymer based on ethyl cellulose and polycaprolactone

Yongkang Bai[a,b], Cheng Jiang[a,b], Qihua Wang[a,*], Tingmei Wang[a]

[a] State Key Laboratory of Solid Lubrication, Lanzhou Institute of Chemical Physics, Chinese Academy of Sciences, Lanzhou 730000, PR China
[b] Graduate University of Chinese Academy of Sciences, Beijing 100039, PR China

ARTICLE INFO

Article history:
Received 7 January 2013
Received in revised form 27 March 2013
Accepted 10 April 2013
Available online 17 April 2013

Keywords:
Ethyl cellulose
Polycaprolactone
Shape memory polymer
Mechanical property
Biomedical suture

ABSTRACT

A novel biological friendly shape memory polymer (SMP) based on ethyl cellulose (EC) and polycaprolactone (PCL) was prepared. The network structure of the polymer was formed by linear EC backbones which were linked by grafted PCL chains, and the results showed outstanding mechanical strength and shape memory property of this polymer. The tensile modulus varied from 104.9 to 373.4 MPa while the tensile strength ranged from 155.4 to 323.6 MPa. And the elongations at break were all above 621%. The shape memory switching temperature could be modulated to 37.2 °C by decreasing the chain length of graft PCL. As EC and PCL are both biodegradable and biocompatible materials, this new polymer has potential application in biomedical field, like biomedical suture, which would be further studied in the future.

1. Introduction

Shape memory polymer (SMP) is a class of smart material which has ability to undergo a large recoverable deformation upon the application of an external stimulus such as heat (Lee, Chun, Chung, Sul, & Cho, 2001; Wang et al., 2011), light (Cheng, Zhang, Yin, & Yu, 2010; Jiang, Kelch, & Lendlein, 2006), electricity (Cho, Kim, Jung, & Goo, 2005; Jung, Yoo, Kim, Cho, & Endo, 2010), magnetism (Schmidt, 2006), water (Zhu et al., 2012). Thereinto, thermally induced SMP is the most extensively investigated group of SMPs. During a shape recovery process of thermally induced SMP, a sample is firstly deformed to a temporary shape under external force at a temperature above transition temperature (T_{tran}, which can be either glass transition temperature T_g, or melting temperature T_m). After being cooled below T_{tran}, this temporary shape could be fixed before removing of external force. Once reheated over T_{tran}, it will recover to original shape again (Behl & Lendlein, 2007; Behl, Razzaq, & Lendlein, 2010; Leng, Lan, Liu, & Du, 2011).

A variety of polymers have been investigated as SMP materials, such as polyurethane (Hearon et al., 2011; Lee, Kim, & Kim, 2004) polyacrylate (Fei, Li, Wu, & Xia, 2012; Yakacki, Satarkar, Gall, Likos, & Hilt, 2009), and polynorbornene (Ahn, Deshmukh, Gopinadhan, Osuji, & Kasi, 2011; Yang, Gao, Zeng, Jiang, & Xie, 2011). However, these materials are neither biodegradable nor biocompatible which limits their application in biomedical field. Polycaprolactone (PCL), a semicrystalline polymer, is widely used as the base material for SMP which is also used in biomedical field for its biocompatibility (Behl, Ridder, Feng, Kelch, & Lendlein, 2009; Deka, Karak, Kalita, & Buragohain, 2010; Lendlein & Kelch, 2002). But the relatively high T_m and poor mechanical property of PCL still limit its potential application in human body (Xue, Dai, & Li, 2009).

Some methods have been reported to decrease the T_m of PCL to body temperature (Ebara, Uto, Idota, Hoffman, & Aoyagi, 2012; Lendlein & Langer, 2002; Xue et al., 2009). Lendlein (Lendlein & Langer, 2002) prepared a linear, phase-segregated multiblock copolymers (oligo (ε-caprolactone) diol, oligo (*p*-dioxanone)diol) because the properties of polymer with this architecture could be tailored by variation of molecular parameters. They successfully prepared a SMP material with T_{tran} of 40 °C and the application of the SMP in organism was also studied. Takao Aoyagi (Ebara et al., 2012) firstly demonstrated that the T_m of PCL materials can be modulated through controlling the branched arm number and molecular weight of PCL. They synthesized two PCL materials cross-linked them together to obtain a material with a T_m of 37.8 °C. And they found the material could really exhibit shape memory effect actuated by body temperature. Mechanical properties of material were also a limiting factor of application of SMP (Voit et al., 2010; Xie, 2010). To improve the mechanical property of SMP, many researches introduced some inorganic nanofillers to polymer materials, such as ZnO (Koerner et al., 2009), SiO_2 (Zhang, Wang, Wang, & Wang, 2011), carbon fillers (Ma et al., 2009). But the harm of these inorganic fillers on human still remain debatable, so a new organic filler was used in this study to solve both of above issues.

* Corresponding author. Tel.: +86 9314968367.
E-mail address: wangqh@licp.cas.cn (Q. Wang).

0144-8617/$ – see front matter © 2013 Elsevier Ltd. All rights reserved.
http://dx.doi.org/10.1016/j.carbpol.2013.04.026

Ethyl cellulose is a kind of cellulose ether which has been widely studied as biomedical or intelligent materials due to its nontoxicity, biocompatibility and high mechanical strength (Bruno, Kasapis, & Heng, 2012; Kang et al., 2006; Shen, Yu, & Huang, 2005; Yu et al., 2012; Yuan, Zhang, Zou, Shen, & Ren, 2012). In this study, ethyl cellulose (EC) was introduced as backbone to polymer network to modulate the T_m and mechanical strength of PCL materials. The ethyl cellulose-polycaprolactone shape memory polymer (EC-SMP) was prepared as follows: (1) firstly, PCL was grafted to EC by ring-opening polymerization (ROP) of epsilon-caprolactone (ε-CL); (2) then the prepolymer (EC-PCL) was cross-linked by diisocyanate. A series of EC-PCL with different molecular weight of graft PCL were prepared through adjusting the ratio between EC and ε-CL. And the T_m was decreased to 37.2 °C after cross-linked reaction when the EC content was at 15 wt%. So the EC-SMP could also exhibit shape memory effect actuated by body temperature. What's more, the introducing of EC to polymer network greatly improved the mechanical strength. Of course, the polymer networks also exhibited well shape memory property.

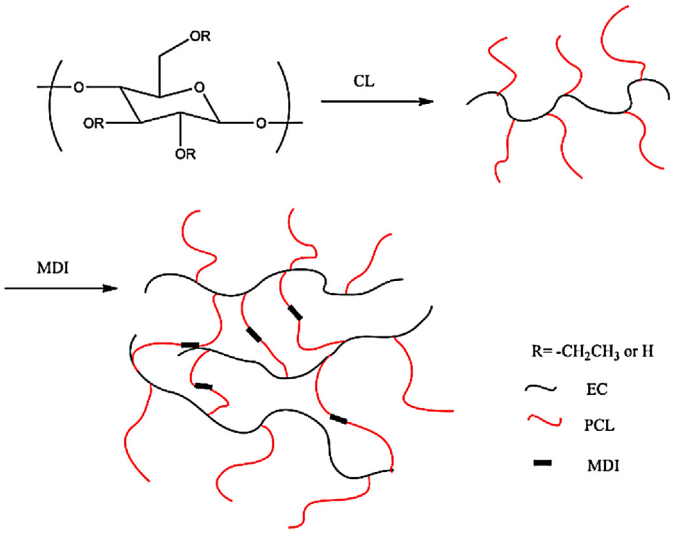

Fig. 1. Synthesis route of EC-SMP.

2. Experiment

2.1. Materials

Ethyl cellulose M70 (M_n = 60,000 g mol^{-1}), stannous octoate was obtained from Sinopharm Chemical Reagent Co., Ltd. Epsilon-caprolactone (ε-CL) and 4,4′-methylenediphenyl diisocyanate (MDI) was received from Acros. All other reagents were bought from Tianjin Chemical Reagents Company. N,N′-dimethylformamide (DMF) and ε-CL were dried with CaH_2 for 24 h and freshly distilled before use.

2.2. Preparation of EC-SMP

A series of EC-SMP with different chain length of graft PCL were prepared by two-step method. Firstly the prepolymer (EC-PCL) was synthesized by ring-opening polymerization (ROP) of ε-CL. A certain amount of EC was dissolved in ε-CL with vigorous stirring at 130 °C under an argon atmosphere. Then 0.5% wt of stannous octoate was added and the mixture was stirred at 130 °C for 12 h. After cooled to room temperature, the resulting polymer was dissolved in dichloromethane and then precipitated from cold *n*-hexane to afford pure graft polymer. The pure polymer was dried in a vacuum oven at 40 °C to a constant mass. Secondly, appropriate amount of EC-PCL and MDI were dissolved in 20 mL DMF and the solution was stirred at 80 °C under protecting of Ar gas until the solution became sticky. Then above product was cast into Teflon plate, followed by further reacting and drying at 80 °C in an oven for 24 h to obtain film sample (the thickness was controlled to be about 0.16 mm). The main synthesis process was shown in Fig. 1.

2.3. Characterization

Fourier transform infrared spectroscopy (FTIR) spectra were recorded on a Bruker IFS 66/s IR spectrophotometer within a range of 4000–600 cm^{-1}. Nuclear magnetic resonance (NMR) spectra were recorded with Advance^{TM}III 400 MHz (Bruker co., Germany) in $CDCl_3$ as solvent and the chemical shifts were calibrated to tetramethylsilane. Scanning electron microscope (SEM) images were taken on a field emission scanning electron microscope (FESEM, JSM-6710F). All samples were coated with gold by sputtering before analyzing.

The thermal properties of polymers were measured with a Mettler Toledo instrument DSC 822 system under a nitrogen atmosphere. For the measurement of samples, samples were heated from 25 to 230 °C, then cooled down to −100 °C, and finally reheated to 230 °C, the heating and cooling rate were both 10 °C/min. Enthalpy change (ΔH_m), melting temperature (T_m) and crystallinity (X_c) were obtained from the second heating curves.

Degree of swelling (Q) and gel content (G) were studied to evaluate the cross-linking degree of grafted polymer networks. To calculate the Q of sample, every sample was swollen in chloroform at 25 °C for 48 h. Samples were weighed before and after swelling. For G, samples were extracted with soxhelt extractor for 24 h by chloroform. And they were calculated according to formulas (1) and (2). ρ_1 and ρ_2 are density of the chloroform and the sample respectively, and the ρ_2 was measured through the Micrometritics Accupyc 1330. m_s is the weight of samples after swelling for 48 h and m_d is the weight of samples after extracting. m_{iso} is the dried weight of samples before swelling and extracting.

$$Q = 1 + \frac{\rho_1}{\rho_2}\left(\frac{m_s}{m_{iso}} - 1\right) \quad (1)$$

$$G = \frac{m_d}{m_{iso}} \quad (2)$$

Tensile tests were performed at a universal testing machine (Shimadzu AG-X) with a strain rate of 20 mm min^{-1}. All specimens were cut to ~20 mm × 3 mm × 0.16 mm for testing and at least five specimens were tested. Shape memory properties was carried out by cyclic thermomechanical tensile and the main process was: (1) heat a sample to T_h (70 °C) and stretch to ε_m; (2) cool to T_l (23 °C); (3) remove the load to obtain the temporary strain $\varepsilon_u(N)$; (3) reheat to T_h and keep at T_h for 5 min to recover the permanent shape $\varepsilon_p(N)$ (N is the number of cycles). (The mainly cycle processing was shown in Fig. S1.) The shape memory property was evaluated by recovery ratio (R_r) and fixing ratio (R_f), and they were calculated as follows:(Lendlein & Kelch, 2002)

$$R_r = \frac{\varepsilon_u(N) - \varepsilon_p(N)}{\varepsilon_u(N) - \varepsilon_p(N-1)} \quad (3)$$

$$R_f = \frac{\varepsilon_u(N)}{\varepsilon_m} \quad (4)$$

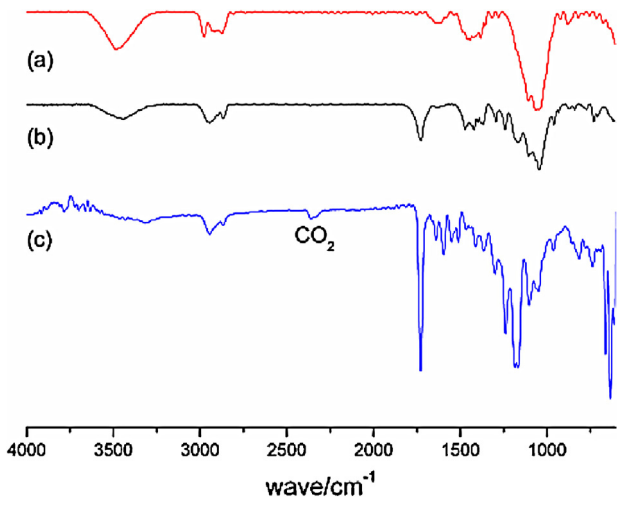

Fig. 2. FTIR spectrum of (a) EC, (b) EC-PCL and (c) EC-SMP.

3. Results and discussion

3.1. Synthesis of EC-SMP

The EC-SMP was prepared by two-step method and the synthesis process was verified by FTIR and ^{1}H NMR (as shown in Figs. 2 and 3). The strong absorption peak at 1065 cm^{-1} in Fig. 2(a) was corresponding to stretching vibration of C—O—C which indicated the cellulose ether of EC. The absorption peak at 3485 cm^{-1} in Fig. 2(a) was attributed to stretching vibration of the remaining —OH on the EC chains which performs as the active center in the following ROP. After ROP of ε-CL, the sharp absorption peak at 1727 cm^{-1} appearing in Fig. 2(b) was attributed to stretching vibration of C=O in PCL and the wide absorption peak at 3437 cm^{-1} suggested the existence of terminal —OH of PCL. Compared to EC, the absorption peak of —OH in PCL moves to lower frequency and was wider due to the stronger interaction of hydrogen bond. The FTIR spectrums (a) and (b) proved that PCL chains were successfully grafted to EC, and the ^{1}H NMR spectrum in Fig. 3 further proved that. The mainly resonance peaks attributed to PCL were marked clearly in the spectrum: 4.03 (t, —CH_2—O—), 2.28 (t, —CH_2—CO—), 1.63 (m, —CH_2—), 1.36 (m, —CH_2—). After reacting with MDI, the peak of —OH disappeared and the wide peak of stretching vibration of —NH appeared at 3320 cm^{-1} in Fig. 2(c). And the absorption peak of C=O in EC-SMP was stronger than that of EC-SMP due to introducing of MDI.

A series of EC-PCL prepolymer with different ratio of EC and PCL were prepared, and the graft length of PCL was estimated by ^{1}H NMR (Xue et al., 2009). The molecular weight (M_n) of graft PCL of each prepolymer was given in Table 1. Then EC-SMP was obtained

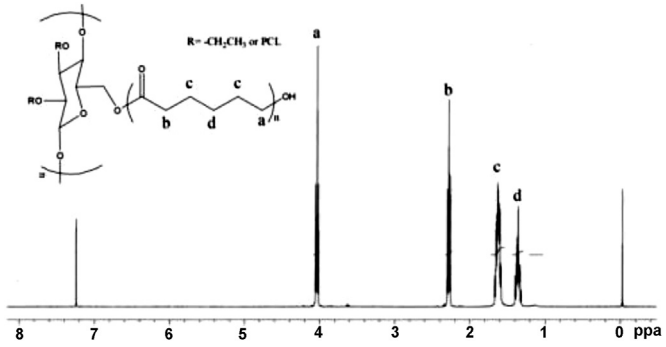

Fig. 3. ^{1}H NMR spectrum of EC-PCL.

Table 1
M_n of grafted PCL, Q and G of EC-SMP.

Sample	M_n (g mol^{-1})	Q (%)	G (%)
EC-SMP-1	11,400	1052 ± 110	59.3 ± 9.9
EC-SMP-2.5	7600	682 ± 52	73.2 ± 2.1
EC-SMP-5	5700	620 ± 70	81.4 ± 1.3
EC-SMP-7.5	2530	518 ± 32	91.0 ± 0.7
EC-SMP-10	2280	472 ± 33	87.5 ± 1.6
EC-SMP-15	1420	312 ± 10	90.5 ± 0.7

by cross-linking with MDI and named as EC-SMP-N (N is related to the weight content of EC in EC-PCL). The values of Q and G were listed in Table 1 to evaluate the cross-linked density of the network structure. In Table 1, Q decreased from 1052% to 312% with the increasing content of EC. The reason for decreasing of Q was that the M_n of PCL was higher with lower content of EC as initiator, so the space in polymer network was larger to allow more solvent entering into polymer network. From Table 1, G had a higher value with low M_n of PCL indicating a higher cross-linking density.

3.2. Thermal and mechanical properties of EC-SMP

The thermal properties of EC-SMP were investigated by differential scanning calorimetry (DSC) to confirm the transition temperature of shape memory process and the results were shown in Table 2. Wherein, X_c was calculated according to the following equation: $X_c = (\Delta H_m/\Delta H_{100\%}) \times 100\%$ ($\Delta H_{100\%}$ is the theoretical heat of fusion of PCL, −135 J g^{-1}) (Nagata and Yamamoto, 2009; Xue et al., 2009). It could be seen in Table 2 that melting temperature (T_m) and crystallinity (X_c) of the EC-SMP and EC-PCL both decreased with the increasing content of EC which should be attributed to the crystalline imperfection of PCL domain. The first factor was the deceasing of M_n of graft PCL which could be easily concluded from Table 2. Moreover, as being the backbone in polymer network, EC was an amorphous polymer which hindered the ordered arrangement of PCL chains during crystallizing process. Furthermore, after cross-linked by MDI, the chain movements of PCL segments were further limited by different EC chains, so the crystallization ability of EC-SMP was weaker than corresponding EC-PCL. And this was extremely obvious when the content of EC reached 15%, X_c and T_m both dropped largely (32.3–8.3% and 53.3–37.2 °C).

Then the mechanical properties of EC-SMP with various molecular weight of graft PCL were studied and the results were shown in Fig. 4. Compared to previous study, the introducing of EC to PCL structure enhanced the stiffness of PCL materials obviously (Lee et al., 2001; Zhang, Giese, Prukop, & Grunlan, 2011). The tensile modulus (E) of all samples was more than 100 MPa due to the reinforcement of EC (E of pure EC is about 507.7 MPa). However, we also found that, when the EC content surpassed 2.5%, the E value of EC-SMP varied from 373.4 to 104.9 MPa with increasing of EC content, which may result from the decreasing of crystallinity of EC-SMP.

Table 2
Thermal properties of EC-SMP and EC-PCL.

EC (%)	EC-SMP			EC-PCL		
	T_m [a] (°C)	ΔH_m [a] (J g^{-1})	X_c [a] (%)	T_m [b] (°C)	ΔH_m [b] (J g^{-1})	X_c [b] (%)
1	55.6	−51.2	37.9	55.9	−58.4	43.3
2.5	55.4	−42.8	31.7	56.4	−55.8	41.4
5	52.4	−39.2	29.0	55.9	−52.2	38.7
7.5	51.6	−39.1	29.0	55.8	−53.4	39.5
10	51.8	−37.8	28.0	55.6	−48.4	35.8
15	37.2	−11.2	8.3	53.3	−43.6	32.3

[a] Represents the relevant parameter of EC-SMP.
[b] Represents the relevant parameter of EC-PCL

Table 3
Shape memory properties of the EC-SMP.[a]

Sample	R_{f1} (%)	R_{f2} (%)	R_{f3-5} (%)	R_{r1} (%)	R_{r2} (%)	R_{r3-5} (%)
EC-SMP-1	99.78 ± 0.38	99.87 ± 0.13	99.88 ± 0.06	91.80 ± 2.47	94.38 ± 3.48	97.89 ± 1.25
EC-SMP-2.5	99.44 ± 0.25	99.63 ± 0.22	99.78 ± 0.07	83.91 ± 0.82	97.05 ± 1.48	98.96 ± 0.18
EC-SMP-5.0	99.22 ± 0.09	98.55 ± 0.65	98.74 ± 0.41	86.48 ± 3.70	97.68 ± 1.08	98.66 ± 0.35
EC-SMP-7.5	98.58 ± 0.42	98.47 ± 0.05	98.49 ± 0.46	87.13 ± 3.30	98.20 ± 0.61	99.72 ± 0.95
EC-SMP-10	97.82 ± 0.86	98.43 ± 1.16	99.10 ± 0.15	73.19 ± 8.55	91.07 ± 10.76	96.04 ± 1.38
EC-SMP-15	71.18 ± 5.25	71.48 ± 3.67	71.76 ± 0.62	60.02 ± 0.39	89.78 ± 5.28	96.21 ± 0.88

[a] R_{fx}, R_{rx}: strain recovery values for the x circle.

The elongation at break (ε) of different EC-SMP presented a similar tendency with the tensile modulus. The ε value reached highest of 1024% at 2.5% then decreased to 621% with the increasing of EC content. In Fig. 4, we can see the elongation at break of pure EC was just about 123%, so it may be the reason for decreasing of elongation at break of EC-SMP after reaching the highest value. Due to the reinforcement EC, the materials also had a very high tensile strength (σ) ranging from 155.4 to 323.6 MPa. And with the increasing of EC content, the σ of EC-SMP became higher gradually until approaching the value of pure EC (331.8 MPa).

Through above analysis, EC-SMP presented excellent mechanical strength due to the high strength of backbone EC in the polymer network. And the SEM images were given to study the morphology of samples. In Fig. S2, EC were dispersed evenly in PCL matrix. The reinforcing mechanism of EC in EC-SMP may be similar to the carbon nanotube composites (Coleman, Khan, & Gun'ko, 2006; Hwang, Shieh, & Hwang, 2004). All EC coated with PCL formed the "sword and sheath" structure in polymer matrix; the interactions between EC and PCL were constituted by around chemical bonds, so the mechanical property was greatly improved.

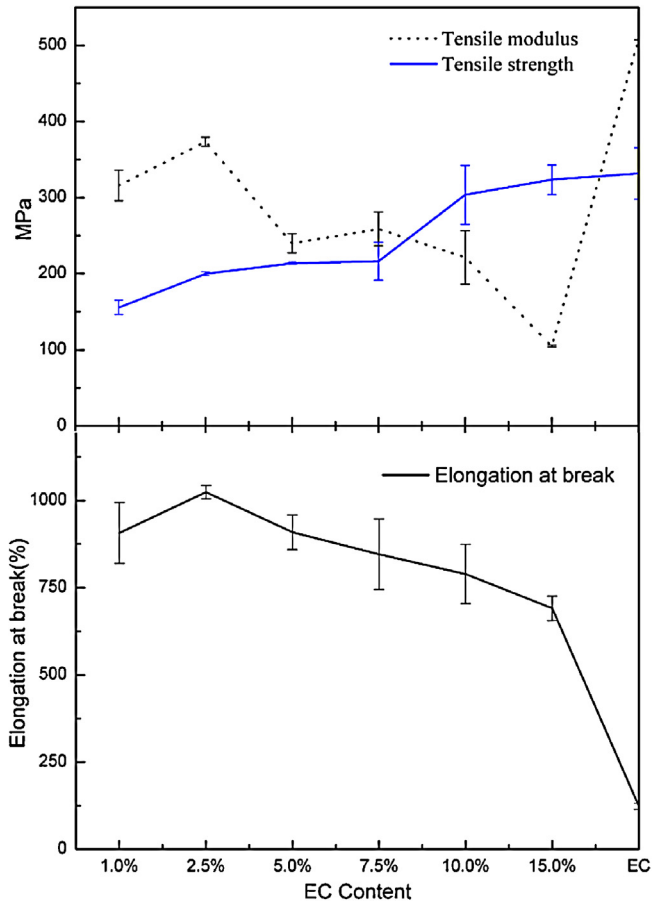

Fig. 4. Mechanical properties of EC-SMP with various weight content of EC.

3.3. Shape memory properties of EC-SMP

The introducing of EC not only enhanced the mechanical strength, but also enabled the materials with excellent shape memory property. A macroscopic shape recovery of the EC-SMP was shown in Fig. S3. The shapes of sample (a) were obtained as follows: after cast into Teflon plate for several hours in oven at 80 °C, the film was taken out and applied appropriate force before reacting absolutely, and then the film was continued to dry to obtain wanted shapes. The materials could recover to the original shape totally after equilibrating at 80 °C.

Furthermore, the R_f and R_r of materials were measured by cyclic thermomechanical tensile tests in two water bathes with different temperature (the strain ratio of all samples was stretched over than 200%). The results were given in Table 3. According to previous studies, the key factor for achieving completely recovery was a fully cross-linked network with cross-linked space which was large and evenly distributed (Lendlein & Kelch, 2002). In our study, PCL chains were grafted to EC chains uniformly, and then it was cross-linked by MDI to form the network structure which meet the request of fully recovery of materials. In Table 3, when the EC content was below 10%, the materials exhibited excellent shape memory property with the R_f values more than 97% and the R_r values more than 96% after 3 cycles. Although the R_f value of EC-SMP-15 was just around 73%, its R_r value was still more than 96% after 3 cycles. In Table 3, we also could find the R_f values decreased with the increasing of EC content which was attributed to the decreasing of crystallinity of PCL. The low crystallinity of materials made the material could not hold innerstress well to keep the temporary shape, so the sample EC-SMP-15 with low crystallinity showed a low value of R_f. Moreover, the R_f values were affected little to the times of cycles while R_r had a relatively low value in first two cycles. The main factor affecting R_f was crystallinity which was affected little to the cycle times, so the R_f values changed little. On the contrary, the R_r values are relatively low in the first two cycles, but exceeded 96% after 3 cycles and preserved at a content value. It may be attributed to the irreversible segment-chain orientation and relaxation effects in polymer network in first two cycles, and the effect of these factors wears off or disappears after 3 cycles (Zhang, Wang, et al., 2011).

According to previous study, tying of a knot with instruments or sutures to close an incision or open lumen was a challengeable operation in endoscopic surgery (Hodgson, Malthaner, & Ostbye, 2000; Hoer, Klinge, Schachtrupp, Tons, & Schumpelick, 2001). Neither too tight nor loose of suture was harm to the healing of wound. Smart surgical suture, which can be actuated by body temperature, may be a possible solution in the future. In our study, EC-SMP with different EC content were prepared, and it can be seen from Table 2 that the melting temperature decreased with increasing of EC content and it declined to 37.2 °C at 15% of EC content. Therefore, the application of EC-SMP as biomedical suture was preliminarily studied and the results were shown in Fig. 5. The sutures were both elongated by 200% first, and then the predesigned shapes were obtained as shown in Fig. 5. After healed to 40 °C, the sutures shrank leading to that the knot was tightened and the "wound" was closed.

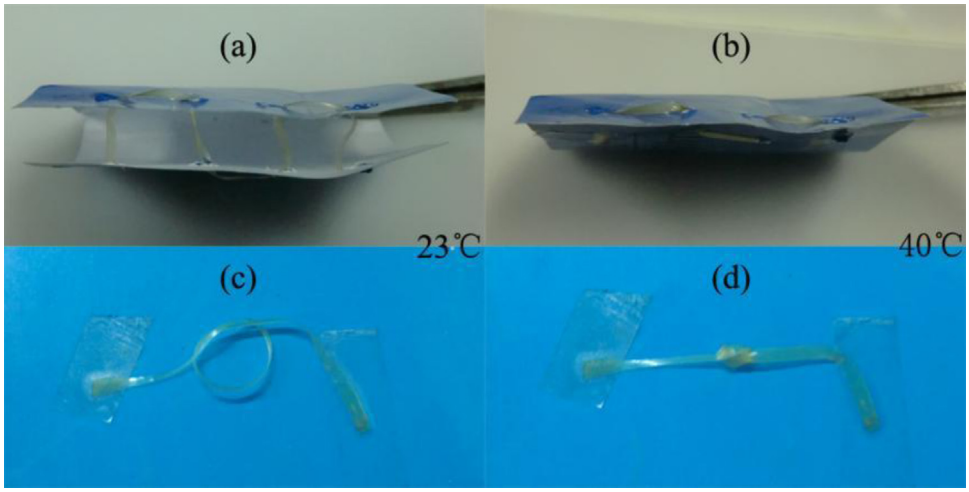

Fig. 5. The study of EC-SMP-15 as suture actuated by 40 °C.

4. Conclusion

In summary, a novel biocompatible ethyl cellulose/polycaprolactone shape memory polymer (EC-SMP) was prepared by two-step method. In this polymer, EC was the backbone of polymer network, and its high mechanical intensity made EC-SMP with outstanding mechanical strength. The tensile modulus of the materials varied from 104.9 to 373.4 MPa while the tensile strength ranged from 155.4 to 323.6 MPa. And the elongations at break of EC-SMP were all more than 621%. Meanwhile, the network structure also made the materials with excellent shape memory property. By tailoring the graft length of polycaprolactone (PCL) in polymer network, the shape memory transition temperature was successfully adjusted near to body temperature. And the materials also exhibited excellent shape memory property actuated by 40 °C as biomedical sutures. Therefore, the biological friendly PCL based shape memory polymer may be able to realize the application in biomaterial development in some degree.

Acknowledgements

The financial supports from the National Science Foundation for Distinguished Young Scholars of China (Grant No. 51025517), the 973 Project of China (2007CB607606) and the National Defense Basic Scientific Research Project (A1320110011) are duly acknowledged.

Appendix A. Supplementary data

Supplementary data associated with this article can be found, in the online version, at http://dx.doi.org/10.1016/j.carbpol.2013.04.026.

References

Ahn, S. K., Deshmukh, P., Gopinadhan, M., Osuji, C. O., & Kasi, R. M. (2011). Side-chain liquid crystalline polymer networks: Exploiting nanoscale smectic polymorphism to design shape-memory polymers. *ACS Nano*, *5*(4), 3085–3095.

Behl, M., & Lendlein, A. (2007). Shape-memory polymers. *Materials Today*, *10*(4), 20–28.

Behl, M., Razzaq, M. Y., & Lendlein, A. (2010). Multifunctional shape-memory polymers. *Advanced Materials*, *22*(31), 3388–3410.

Behl, M., Ridder, U., Feng, Y., Kelch, S., & Lendlein, A. (2009). Shape-memory capability of binary multiblock copolymer blends with hard and switching domains provided by different components. *Soft Matter*, *5*(3), 676–684.

Bruno, L., Kasapis, S., & Heng, P. W. S. (2012). Effect of polymer molecular weight on the structural properties of non aqueous ethyl cellulose gels intended for topical drug delivery. *Carbohydrate Polymers*, *88*(1), 382–388.

Cheng, F. T., Zhang, Y. Y., Yin, R. Y., & Yu, Y. L. (2010). Visible light induced bending and unbending behavior of crosslinked liquid-crystalline polymer films containing azotolane moieties. *Journal of Materials Chemistry*, *20*(23), 4888–4896.

Cho, J. W., Kim, J. W., Jung, Y. C., & Goo, N. S. (2005). Electroactive shape-memory polyurethane composites incorporating carbon nanotubes. *Macromolecular Rapid Communications*, *26*(5), 412–416.

Coleman, J. N., Khan, U., & Gun'ko, Y. K. (2006). Mechanical reinforcement of polymers using carbon nanotubes. *Advanced Materials*, *18*(6), 689–706.

Deka, H., Karak, N., Kalita, R. D., & Buragohain, A. K. (2010). Biocompatible hyperbranched polyurethane/multi-walled carbon nanotube composites as shape memory materials. *Carbon*, *48*(7), 2013–2022.

Ebara, M., Uto, K., Idota, N., Hoffman, J. M., & Aoyagi, T. (2012). Shape-memory surface with dynamically tunable nano-geometry activated by body heat. *Advanced Materials*, *24*(2), 273–278.

Fei, G., Li, G., Wu, L., & Xia, H. (2012). A spatially and temporally controlled shape memory process for electrically conductive polymer–carbon nanotube composites. *Soft Matter*, *8*, 5123–5126.

Hearon, K., Gall, K., Ware, T., Maitland, D. J., Bearinger, J. P., & Wilson, T. S. (2011). Post-polymerization crosslinked polyurethane shape memory polymers. *Journal of Applied Polymer Science*, *121*(1), 144–153.

Hodgson, N. C. F., Malthaner, R. A., & Ostbye, T. (2000). The search for an ideal method of abdominal fascial closure – a meta-analysis. *Annals of Surgery*, *231*(3), 436–442.

Hoer, J., Klinge, U., Schachtrupp, A., Tons, C., & Schumpelick, V. (2001). Influence of suture technique on laparotomy wound healing: An experimental study in the rat. *Langenbecks Archives of Surgery*, *386*(3), 218–223.

Hwang, G. L., Shieh, Y. T., & Hwang, K. C. (2004). Efficient load transfer to polymer-grafted multiwalled carbon nanotubes in polymer composites. *Advanced Functional Materials*, *14*(5), 487–491.

Jiang, H. Y., Kelch, S., & Lendlein, A. (2006). Polymers move in response to light. *Advanced Materials*, *18*(11), 1471–1475.

Jung, Y. C., Yoo, H. J., Kim, Y. A., Cho, J. W., & Endo, M. (2010). Electroactive shape memory performance of polyurethane composite having homogeneously dispersed and covalently crosslinked carbon nanotubes. *Carbon*, *48*(5), 1598–1603.

Kang, H., Liu, W., He, B., Shen, D., Ma, L., & Huang, Y. (2006). Synthesis of amphiphilic ethyl cellulose grafting poly(acrylic acid) copolymers and their self-assembly morphologies in water. *Polymer*, *47*(23), 7927–7934.

Koerner, H., Kelley, J., George, J., Drummy, L., Mirau, P., Bell, N. S., et al. (2009). ZnO nanorod-thermoplastic polyurethane nanocomposites: Morphology and shape memory performance. *Macromolecules*, *42*(22), 8933–8942.

Lee, B. S., Chun, B. C., Chung, Y. C., Sul, K. I., & Cho, J. W. (2001). Structure and thermomechanical properties of polyurethane block copolymers with shape memory effect. *Macromolecules*, *34*(18), 6431–6437.

Lee, S. H., Kim, J. W., & Kim, B. K. (2004). Shape memory polyurethanes having crosslinks in soft and hard segments. *Smart Materials and Structures*, *13*(6), 1345–1350.

Lendlein, A., & Kelch, S. (2002). Shape-memory effect. *Angewandte Chemie International Edition*, *41*, 2034–2057.

Lendlein, A., & Langer, R. (2002). Biodegradable, elastic shape-memory polymers for potential biomedical applications. *Science*, *296*(5573), 1673–1676.

Leng, J., Lan, X., Liu, Y., & Du, S. (2011). Shape-memory polymers and their composites: Stimulus methods and applications. *Progress in Materials Science*, *56*(7), 1077–1135.

Ma, W., Liu, L., Zhang, Z., Yang, R., Liu, G., Zhang, T., et al. (2009). High-strength composite fibers: Realizing true potential of carbon nanotubes in polymer matrix through continuous reticulate architecture and molecular level couplings. *Nano Letters*, *9*(8), 2855–2861.

Nagata, M., & Yamamoto, Y. (2009). Synthesis and characterization of photocrosslinked poly(epsilon-caprolactone)s showing shape-memory properties. *Journal of Polymer Science Part A: Polymer Chemistry*, *47*(9), 2422–2433.

Schmidt, A. M. (2006). Electromagnetic activation of shape memory polymer networks containing magnetic nanoparticles. *Macromolecular Rapid Communications*, *27*(14), 1168–1172.

Shen, D. W., Yu, H., & Huang, Y. (2005). Densely grafting copolymers of ethyl cellulose through atom transfer radical polymerization. *Journal of Polymer Science Part A: Polymer Chemistry*, *43*(18), 4099–4108.

Voit, W., Ware, T., Dasari, R. R., Smith, P., Danz, L., Simon, D., et al. (2010). High-strain shape-memory polymers. *Advanced Functional Materials*, *20*(1), 162–171.

Wang, Z., Hansen, C., Ge, Q., Maruf, S. H., Ahn, D. U., Qi, H. J., et al. (2011). Programmable, pattern-memorizing polymer surface. *Advanced Materials*, *23*(32), 3669–3673.

Xie, T. (2010). Tunable polymer multi-shape memory effect. *Nature*, *464*(7286), 267–270.

Xue, L., Dai, S. Y., & Li, Z. (2009). Synthesis and characterization of three-arm poly(epsilon-caprolactone)-based poly(ester-urethanes) with shape-memory effect at body temperature. *Macromolecules*, *42*(4), 964–972.

Yakacki, C. M., Satarkar, N. S., Gall, K., Likos, R., & Hilt, J. Z. (2009). Shape-memory polymer networks with Fe_3O_4 nanoparticles for remote activation. *Journal of Applied Polymer Science*, *112*(5), 3166–3176.

Yang, D., Gao, D. Y., Zeng, C., Jiang, J. S., & Xie, M. R. (2011). POSS-enhanced shape-memory copolymer of polynorbornene derivate and polycyclooctene through ring-opening metathesis polymerization. *Reactive & Functional Polymers*, *71*(11), 1096–1101.

Yu, Y. L., Zhang, M. J., Xie, R., Ju, X. J., Wang, J. Y., Pi, S. W., et al. (2012). Thermo-responsive monodisperse core-shell microspheres with PNIPAM core and biocompatible porous ethyl cellulose shell embedded with PNIPAM gates. *Journal of Colloid and Interface Science*, *376*, 97–106.

Yuan, W., Zhang, J., Zou, H., Shen, T., & Ren, J. (2012). Amphiphilic ethyl cellulose brush polymers with mono and dual side chains: Facile synthesis, self-assembly, and tunable temperature–pH responsivities. *Polymer*, *53*(4), 956–966.

Zhang, D. W., Giese, M. L., Prukop, S. L., & Grunlan, M. A. (2011). Poly(epsilon-caprolactone)-based shape memory polymers with variable polydimethylsiloxane soft segment lengths. *Journal of Polymer Science Part A: Polymer Chemistry*, *49*(3), 754–761.

Zhang, Y., Wang, Q., Wang, C., & Wang, T. (2011). High-strain shape memory polymer networks crosslinked by SiO_2. *Journal of Materials Chemistry*, *21*(25), 9073–9078.

Zhu, Y., Hu, J. L., Luo, H. S., Young, R. J., Deng, L. B., Zhang, S., et al. (2012). Rapidly switchable water-sensitive shape-memory cellulose/elastomer nanocomposites. *Soft Matter*, *8*(8), 2509–2517.